

**DTIC FILE COPY**

WRDC-TR-90-2008

**AD-A226 944**



**EFFECT OF INTERLINE HEAT FLOW PARAMETER ON CONTACT  
LINE HEAT TRANSFER**

Peter C. Wayner, Jr.

Rensselaer Polytechnic Institute  
Department of Chemical Engineering  
Troy, NY 12180-3590

April 1990

Interim Report for Period April 1988 - June 1989

Approved for public release; distribution is unlimited

**DTIC**  
**ELECTE**  
**SEP 27 1990**  
**CS**  
**E** **D**

AEROPROPULSION AND POWER LABORATORY  
WRIGHT RESEARCH AND DEVELOPMENT CENTER  
AIR FORCE SYSTEMS COMMAND  
WRIGHT-PATTERSON AIR FORCE BASE, OHIO 45433-6563

## NOTICE

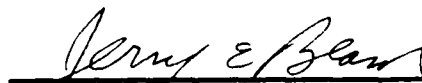
WHEN GOVERNMENT DRAWINGS, SPECIFICATIONS, OR OTHER DATA ARE USED FOR ANY PURPOSE OTHER THAN IN CONNECTION WITH A DEFINITELY GOVERNMENT-RELATED PROCUREMENT, THE UNITED STATES GOVERNMENT INCURS NO RESPONSIBILITY OR ANY OBLIGATION WHATSOEVER. THE FACT THAT THE GOVERNMENT MAY HAVE FORMULATED OR IN ANY WAY SUPPLIED THE SAID DRAWINGS, SPECIFICATIONS, OR OTHER DATA, IS NOT TO BE REGARDED BY IMPLICATION, OR OTHERWISE IN ANY MANNER CONSTRUED, AS LICENSING THE HOLDER, OR ANY OTHER PERSON OR CORPORATION; OR AS CONVEYING ANY RIGHTS OR PERMISSION TO MANUFACTURE, USE, OR SELL ANY PATENTED INVENTION THAT MAY IN ANY WAY BE RELATED THERETO.

THIS REPORT HAS BEEN REVIEWED BY THE OFFICE OF PUBLIC AFFAIRS (ASD/PA) AND IS RELEASABLE TO THE NATIONAL TECHNICAL INFORMATION SERVICE (NTIS). AT NTIS IT WILL BE AVAILABLE TO THE GENERAL PUBLIC INCLUDING FOREIGN NATIONS.

THIS TECHNICAL REPORT HAS BEEN REVIEWED AND IS APPROVED FOR PUBLICATION.




WON S. CHANG  
Project Engineer



JERRY E. BEAM, TAM  
Power Technology Branch  
Aerospace Power Division  
Aero Propulsion and Power Laboratory

FOR THE COMMANDER



WILLIAM U. BORGER  
Chief, Aerospace Power Division  
Aero Propulsion & Power Laboratory

IF YOUR ADDRESS HAS CHANGED, IF YOU WISH TO BE REMOVED FROM OUR MAILING LIST, OR IF THE ADDRESSEE IS NO LONGER EMPLOYED BY YOUR ORGANIZATION PLEASE NOTIFY WRDC/POOS-3, WRIGHT-PATTERSON AFB, OH 45433-6563 TO HELP MAINTAIN A CURRENT MAILING LIST.

COPIES OF THIS REPORT SHOULD NOT BE RETURNED UNLESS RETURN IS REQUIRED BY SECURITY CONSIDERATIONS, CONTRACTUAL OBLIGATIONS, OR NOTICE ON A SPECIFIC DOCUMENT.

REPORT DOCUMENTATION PAGE				Form Approved OMB No 0704-0188	
1a. REPORT SECURITY CLASSIFICATION Unclassified			1b. RESTRICTIVE MARKINGS		
2a. SECURITY CLASSIFICATION AUTHORITY			3. DISTRIBUTION/AVAILABILITY OF REPORT Approved for public release, Distribution is unlimited.		
2b. DECLASSIFICATION/DOWNGRADING SCHEDULE					
4. PERFORMING ORGANIZATION REPORT NUMBER(S) RPI-CHE/PCW-89-01			5. MONITORING ORGANIZATION REPORT NUMBER(S) WRDC-TR-90-2008		
6a. NAME OF PERFORMING ORGANIZATION Rensselaer Polytechnic Institute		6b. OFFICE SYMBOL (If applicable)	7a. NAME OF MONITORING ORGANIZATION Wright Research and Development Center Aero-Propulsion & Power Laboratory(WRDC/POOS)		
6c. ADDRESS (City, State, and ZIP Code) Department of Chemical Engineering Troy, NY 12180-3590			7b. ADDRESS (City, State, and ZIP Code) Wright-Patterson AFB, OH 45433-6563		
8a. NAME OF FUNDING / SPONSORING ORGANIZATION		8b. OFFICE SYMBOL (If applicable)	9. PROCUREMENT INSTRUMENT IDENTIFICATION NUMBER F33615-88-C-2821		
8c. ADDRESS (City, State, and ZIP Code)			10. SOURCE OF FUNDING NUMBERS		
			PROGRAM ELEMENT NO. 63321C	PROJECT NO. 0581	TASK NO. 20
11. TITLE (Include Security Classification) EFFECT OF INTERLINE HEAT FLOW PARAMETER ON CONTACT LINE HEAT TRANSFER					
12. PERSONAL AUTHOR(S) Wayner, Peter C., Jr.					
13a. TYPE OF REPORT Interim		13b. TIME COVERED FROM 88 April TO 89 June		14. DATE OF REPORT (Year, Month, Day) April 1990	
15. PAGE COUNT 36					
16. SUPPLEMENTARY NOTATION					
17. COSATI CODES			18. SUBJECT TERMS (Continue on reverse if necessary and identify by block number)		
FIELD	GROUP	SUB-GROUP	Capillary pressure, evaporation, disjoining pressure, thin liquid film, interfacial phenomena		
19. ABSTRACT (Continue on reverse if necessary and identify by block number) A circular heat transfer cell was designed and fabricated to study fluid flow and change of phase heat transfer in the contact line region. The cell incorporates the use of ellipsometry and interferometry to measure ultra-thin film thickness profiles, which give the local pressure field for fluid flow. In addition, the total fluid flow rate and, therefore, the integral heat sink of the evaporating meniscus can be measured. A theoretical equation that includes the effects of capillarity, disjoining pressure, gravity and temperature on the thin film heat transfer process has been developed and used.					
20. DISTRIBUTION/AVAILABILITY OF ABSTRACT <input checked="" type="checkbox"/> UNCLASSIFIED/UNLIMITED <input type="checkbox"/> SAME AS RPT <input type="checkbox"/> DTIC USERS			21. ABSTRACT SECURITY CLASSIFICATION Unclassified		
22a. NAME OF RESPONSIBLE INDIVIDUAL Dr. Won S. Chang			22b. TELEPHONE (Include Area Code) 513-255-2922		22c. OFFICE SYMBOL WRDC/POOS

# TABLE OF CONTENTS

	Page
INTRODUCTION	1
EXPERIMENTAL: GENERAL	2
EXPERIMENTAL: DESCRIPTION OF THE CELL	3
EXPERIMENTAL: CLEANING	4
EXPERIMENTAL: COMPLEMENTARY CLEANING STUDIES	5
EXPERIMENTS	6
THEORETICAL	7
CURRENT STATUS OF PRESENTATIONS AND PUBLICATIONS	8
APPENDICES	
A - THE EFFECT OF INTERFACIAL MASS TRANSPORT ON FLOW IN THIN LIQUID FILMS	A-1
B - HEAT TRANSFER AND FLUID FLOW IN AN EVAPORATING EXTENDED MENISCUS	B-1

For	
<input checked="checked" type="checkbox"/>	
<input type="checkbox"/>	
Unprocessed	
Distillation	
By	
Distribution/	
Availability Codes	
Dist	Avail and/or Special
A-1	



## INTRODUCTION

The long range objectives of this research are to identify and correlate important properties of the heat transfer process that can be used to optimize the heat sink capabilities of evaporating thin films. Initially, we proposed to emphasize the "Interline Heat Flow Parameter". Using the results of our theoretical research we now plan to enhance this objective and include the evaluation of the "Capillary Pumping Parameter" for completeness. The interline heat flow parameter is important in ultra-thin films where the liquid-solid interfacial force field predominates, whereas the capillary pumping parameter is important in thicker films.

$$Q = \left( \frac{\gamma \Delta h}{v} \right) \frac{\delta^3 K'}{3} + \left( \frac{\bar{A} \Delta h}{v} \right) \frac{\delta'}{\delta} \quad (1)$$

where

$2\pi\bar{A}$  is the Hamaker constant,

$\delta$  is the thickness of the liquid film,

$\Delta h$  is the heat of vaporization,

$\gamma$  is the surface tension,

$K'$  is the curvature gradient,

$v$  is the kinematic viscosity,

$\frac{\gamma \Delta h}{v}$  is the capillary pumping parameter,

$\frac{\bar{A} \Delta h}{v}$  is the interline heat flow parameter,

with  $K'$  and  $\delta'$  evaluated at  $\delta(x)$ .

Therefore, the experimentally measured film thickness profile can be used to calculate the integral heat sink.

There are two main aspects of the program: experimental and theoretical. We will discuss the experimental portion first by outlining significant decisions and accomplishments that have occurred during the first 16 months. This will be followed by a discussion of the theoretical accomplishments.

## **EXPERIMENTAL: GENERAL**

The major experimental task completed during this period was the design and fabrication of a heat transfer cell for studying thin film heat transfer and fluid flow in the contact line region. A considerable amount of effort was directed at designing and testing a new capillary feeder for the heat transfer cell. This concept was tested with various flow geometries and it was found that a circular capillary feeder works best in terms of flow symmetry, absence of "edge effects", efficient sealing, and symmetrical temperature and heat flux profiles. We have decided to evaluate the integral evaporation rate in the contact line region by measuring the total fluid flow rate from the capillary feeder and evaluating this in light of the measured thickness profile using Eq. (1). This eliminates recondensation uncertainty. Fig. 1 is a schematic view of the circular capillary feeder without its enclosure. A photograph of the complete cell is given in Fig. 2.

Both the ultra thin ( $\delta < 20$  nm) and the thin film ( $\delta > 20$  nm) regions of an evaporating liquid film on a standard surface (bare Si wafer) can be studied using two different optical techniques, ellipsometry and interferometry. The advantage of this particular cell is its flexibility - both the ellipsometer and the high power interferometer can be used separately or, for some magnifications, simultaneously and specific design features allow high heat flux studies.

The cell is basically a miniature capillary feeder, the liquid spreads towards the hot spot, gets evaporated and is replenished from the upstream source by the action of capillary suction and disjoining pressure. The cell has the provision of feeding liquid from outside and the feeding rate will be monitored to evaluate the integral evaporation rate for a particular power input. The heat source is a circular Platinum

heater located at the center of the substrate. The temperature profile will be measured by using small thermocouples attached at the back of the substrate. We have decided to use thermocouples instead of Silicon Carbide thermistor arrays because a current doctoral thesis in our program by E. Kiewra demonstrated that there is virtually no difference in the temperature data collected by these two different methods. Therefore, the added complexity associated with the thermistors is not rewarded by improved understanding.

Another crucial factor in determining the stability and equilibrium configuration of the liquid meniscus on the Silicon surface is the cleanliness and liquid purity. The cleaning and the liquid purification procedures will be discussed in the next section. An important feature of this cell is that it can be evacuated to a high vacuum. This will reduce the water vapor (which, if present with organic test fluids, can affect the interfacial force field) adsorbed on the inner surface of the cell walls.

#### **EXPERIMENTAL: DESCRIPTION OF THE CELL**

The substrate of the cell is a single crystal Silicon wafer  $7.6 \times 10^{-2}$  m in diameter and about  $4 \times 10^{-4}$  m thick. The Silicon substrate has a high degree of surface uniformity, high reflectivity and its optical and physical properties are well known. In the future it will be possible to use micromachining techniques on the Silicon wafer to make micro-grooves to increase the contact line length and thereby enhance the heat transfer process. The heat source is a circular shaped heater at the center of the wafer made by painting and baking a Platinum compound at the backside of the wafer. Chromel-Alumel (type K) thermocouples are attached along the centerline on the backside of the substrate.

Fig. 2 shows a photograph of the cell. The cell consists of three parts. The top part is a hollow prism milled from a solid Aluminum block. The two sides are at an angle of  $70^\circ$  with the horizontal. This is the optimum angle of incidence for ellipsometric measurements. Each side contains two viewing ports - supplied by MDC Vacuum Corporation, made of 7056 glass and they are bakeable to relieve residual

stresses. The viewpoints are mounted on three inches long nipples to keep them away from the evaporation areas and thereby minimizing condensation on them. The top contains another viewpoint for viewing the liquid level in the active areas so that the evaporation rate can be determined while the process is going on. It also has a connection for a vacuum line, Nitrogen supply and a feeding system. The second part is an adjustable hollow cylinder which fits the hole in the top portion of the prism with matching threads. During interferometric studies this part can reach very close to the substrate surface. The microscope objective goes into the cylinder. The objective is separated from the inside atmosphere by a heated glass plate. To allow unobstructed laser light to enter during the ellipsometric studies this assembly can be lifted using the threads. This feature enables the use of both the ellipsometer and the high power microscope for interferometry. The third part consists of an Aluminum plate which is carefully machined to form the capillary groove. The groove holds and feeds liquid to the circular meniscus. The Silicon plate rests in between the Aluminum plate and a Teflon plate - secured in place tightly by a Teflon-coated O-ring and a set of 12 screws. Beneath the Teflon plate is a thick Aluminum base plate which holds the top prism and the inside parts. A hole runs between this plate and the Teflon plate to reach the Silicon wafer to allow easy passage of thermocouple and heat source wires. The end of the hole has the provision for a screwed in cap which is kept closed during vacuum operation for cleaning. The vacuum line and the Nitrogen line are connected to the cell by a three way valve. During vacuum operation the Nitrogen line is kept closed. Subsequently, we close the vacuum line and the Nitrogen valve is opened slowly to feed extra-dry grade Nitrogen inside the cell for operation at a positive gauge pressure. The positive gauge pressure minimizes the diffusion of impurities into the cell.

#### **EXPERIMENTAL: CLEANING**

Cleaning of the cell assembly and particularly the Silicon wafer is very critical to obtaining reliable experimental data. The Silicon substrate is very sensitive to its cleaning procedure and the equilibrium film thickness is a function of its cleaning



history. For our purpose the term "cleanliness" is defined as the minimization of any dust particles on the Silicon surface or cell surroundings, a well characterized Silicon surface (presence of oxide, absence of any organic layers etc.) and the absence of anything which may contaminate the liquid. We will use a standard cleaning procedure before each and every experiment so that the substrate properties will remain constant. We are also evaluating different cleaning processes and a liquid purification system which will be discussed later.

We will describe our standard cleaning process first. The Cell is first rinsed well with DI water, then immersed in pure Ethanol and put in an ultrasonic bath for about half an hour. It is then blow dried inside a class-100 clean hood, rinsed with the test fluid and dried in an oven at 150°C. The substrate is dipped into dilute Hydrofluoric acid to remove any built up oxide, rinsed with DI water, test fluid and then blow dried inside a class-100 hood using pure and dry Nitrogen. One point to note here is that Silicon always has a native oxide of about 30 Å thickness. Once the cell parts and substrate are dry they are assembled and mounted on the scanning stage. An appropriate amount of test fluid is then introduced through the feed port to form the meniscus. The system is left to equilibrate with the surrounding for at least half a day before taking any measurements. At this point the Hamaker constant can be measured to characterize the surface.

The cell can be evacuated to a high vacuum by bringing the cell pressure down to 50 milli-torr. Pulling a high vacuum inside the cell and then breaking the vacuum using dry Nitrogen may prove to be an improvement over the above described cleaning process. This possibility will be explored at a later stage.

### **EXPERIMENTAL: COMPLEMENTARY CLEANING STUDIES**

To investigate the effects of cleanliness and in the process define the term itself more precisely, we designed a simpler glass cell which can be cleaned more thoroughly and which allows the effect of different cleaning steps to be monitored and controlled. The quartz glass cell was constructed with a ground glass joint at one

end, so that a dessicant section can be attached to preferentially adsorb the water vapor. The need for windows and O-rings was eliminated so that the simple glass cell can be easily cleaned and baked. A liquid purification and filtration column can also be attached for feeding purified, filtered liquid into the cell. The liquid can be purified by passing it through a column of silica-gel and alumina to remove the aqueous and polar impurities and then through a membrane filter with a pore size of 0.2  $\mu\text{m}$ .

Briefly the following cleaning procedure will be evaluated: All glass parts including the cell, dessicant, feed and purification sections will be rinsed in an ultrasonic chamber with soap solution followed by repeated rinsing with purified distilled water. They will be dried in a stream of pure filtered Nitrogen, rinsed with pure filtered fluid, dried and then baked at 250°C for 1 hr. The wafer will be treated with dilute HF (1:100) and then rinsed with deionized water, dried with Nitrogen, rinsed with pure filtered liquid, dried and then baked with the cell. The dessicant section will be attached during the baking. The cell will then be cooled with the dessicant section still attached. Then the cell will be irradiated by short wavelength UV light (184 nm and 257 nm) to clean the Silicon surface of adsorbed organic impurities. This treatment is presumed to leave behind a clean, oxidized surface. Purified, filtered liquid can now be introduced into the cell. The importance and effect of various cleaning variables will be investigated. Further cleaning procedures like creating an inert atmosphere or vacuum in the cell are also under consideration. All these cleaning steps will be performed in a controlled dust free atmosphere.

## **EXPERIMENTS**

In this section we describe how we measure the different quantities in Eq. (1), namely  $\delta(x)$ ,  $\bar{A}$  experimentally. The film thickness profiles of the liquid on the substrate are measured using interferometry and/or ellipsometry. Both of these two methods are well established (J.G. Truong and P.C. Wayner, Jr., *J. Chem. Phys.*, **87**, pp. 4180-4188, 1987), so a detailed discussion is not included herein. We have successfully tested the performance of our cell with these two optical techniques.  $\delta(x)$

is measured as a function of power input and fluid properties.  $A$  can be determined by analyzing the ultra-thin film section under isothermal condition. Together they allow us to calculate the integral heat sink,  $Q$ , for the region  $\delta(x) > 0$  (from Eq. (1)). An independent measurement of  $Q$  for the total meniscus region is obtained by measuring the total amount of fluid evaporated over a given period of time. These two sets of data will be analyzed in light of each other.

The temperature profiles will be obtained using the thermocouples attached to the bottom of the substrate. The interline heat flow parameter,  $\frac{\dot{A}\Delta h}{v}$ , and  $\frac{\gamma\Delta h}{v}$  will also be evaluated and their effect on fluid flow and heat transfer in the contact line region studied. From the film thickness profile we can determine the evaporative mass flux leaving the surface.

## **THERORETICAL**

One of the major theoretical results to date is Eq. (37) in Appendix A entitled "The Effect of Interfacial Mass Transport on Flow in Thin Liquid Films". The equation includes the combined effects of capillarity (therefore, the capillary pumping parameter), disjoining pressure (therefore, the interline heat flow parameter), gravity and temperature on fluid flow and heat transfer in the contact line region. Since both the interline heat flow parameter and the capillary pumping parameter are present in this equation their complementary effects can be evaluated. When the right hand side and the left hand side of Eq. (37) are not equal, the terms in the equation can be used with Eq. (1) in the same paper to analyze the transient case. Therefore we have been able to formulate a comprehensive equation for general use. A paper detailing numerical results based on a simpler version of Eq. (37) (i.e., a horizontal film in which gravitational effects are neglected) is being proposed for presentation at the 9th International Heat Transfer Conference. Appendix B is a paper entitled "Heat Transfer and Fluid Flow in an Evaporating Extended Meniscus". A note based on only the disjoining pressure portion of this equation entitled "A Dimensionless Number for the Contact Line Heat Sink" was published by the *ASME Journal of Heat Transfer* (Vol.

111, 813-814, 1989). Finally, we note that since the theoretical analysis includes gravity and film tension (along with surface tension) the results are very comprehensive.

Further use of this equation will, of course, be directed at evaluating the results of our experimental program.

### **CURRENT STATUS OF PRESENTATIONS AND PUBLICATIONS**

- 1) Wayner, P.C., Jr., "The Effect of Interfacial Mass Transport on Flow in Thin Liquid Films", presented at the International Symposium on Thin Solid and Liquid Films, University of Bristol, England, 11-13 September 1989. Preliminary copy attached; to be published in *Colloids and Surfaces*.
- 2) Wayner, Jr., P.C., Jr. and J. Schonberg, "Heat Transfer and Fluid Flow in an Extended Meniscus," to be presented at the 9th International Heat Transfer Conference, Israel, August 1990. Preliminary copy attached.
- 3) Wayner, P.C., Jr., "A Dimensionless Number for Heat Transfer in the Contact Line Region," *ASME J. of Heat Transfer*, Vol. 111, 1989, pp. 813-814.
- 4) Sujanani, M. and P.C. Wayner, Jr., "Spreading at the Solid-Liquid-Vapor Interline," paper presented at the 10th Symposium on Thermophysical Properties, National Bureau of Standards, Gaithersburg, MD, June 20-23, 1988. (This presentation was concerned with the characterization of the substrate surface and simple fluid flow models.)

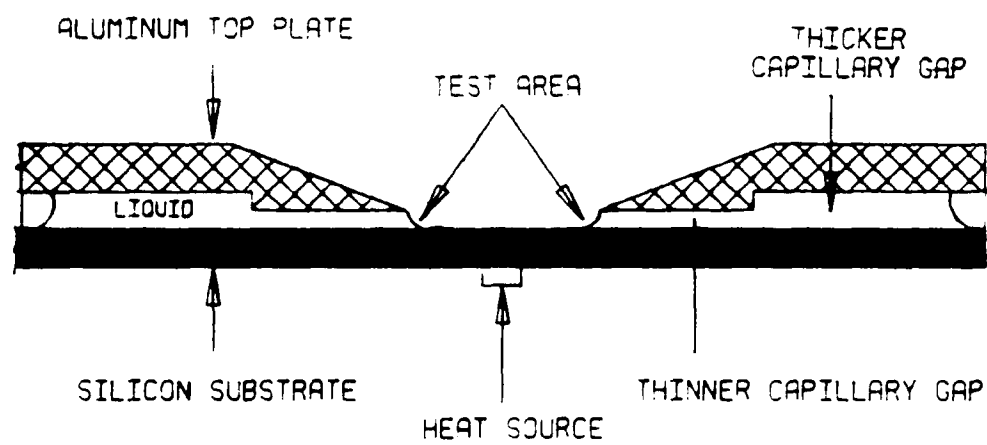


FIG.-1 CIRCULAR CAPILLARY FEEDER

APPENDIX A

THE EFFECT OF INTERFACIAL MASS TRANSPORT ON FLOW IN THIN LIQUID FILMS

For "Thin Film - Special Issue" of Colloids and Surfaces. Paper presented at  
International Symposium on Thin Solid and Liquid Films  
University of Bristol, Bristol, England  
11-13 September, 1989  
(Revised 2/1990)

## THE EFFECT OF INTERFACIAL MASS TRANSPORT ON FLOW IN THIN LIQUID FILMS

Peter C. Wayner, Jr.  
Department of Chemical Engineering  
Rensselaer Polytechnic Institute  
Troy, NY 12180-3590, USA

The equilibrium thermodynamics and the dynamics of flow in an extended meniscus that includes both the relatively thick film region controlled by capillarity and the ultra-thin film region controlled by the liquid-solid-vapor interfacial force field are analyzed. The effects of capillarity, disjoining pressure, gravity and temperature on equilibrium, fluid flow and mass transfer associated with the liquid film are discussed. The non-equilibrium processes of change-of-phase heat transfer and fluid flow in stationary and in spreading thin films are intrinsically connected because of their common dependence on the intermolecular force field and gravity. Criteria to determine the relative importance of fluid flow and interfacial mass transfer based on the film profile and the thermophysical properties of the system are developed. An evaporation/condensation mechanism is found to be important in contact line motion.

$$d \ln f = \frac{d\gamma^f}{RT\delta\Delta n} - \frac{\Delta s}{RT\Delta n} dT \quad (9)$$

Derjaguin and Zorin [5] essentially used Eq. (9) to study adsorption on a superheated solid surface placed close to but slightly above a pool of liquid. Using Eq. (9) with  $d \ln f = 0$  and Eq. (7) for  $d\gamma^f$  gives

$$d\Pi = (s_v - s_l)dT \quad (10)$$

Integration of Eq. (10) over a small temperature change ( $T_v, \Pi = 0; T_{lv}, \Pi$ ) during which  $(s_v - s_l)$  is approximately constant leads to

$$\Pi = (s_v - s_l) (T_{lv} - T_v) \quad (11)$$

Using  $\Pi = -A/6\pi\delta^3$  for film thicknesses less than 20 nm and  $(s_v - s_l) = \Delta h/T_i$ , where  $T_i = (T_{lv} + T_v)/2$ ,

$$\delta = \left( \frac{-AT_i}{6\pi(T_{lv} - T_v)\Delta h} \right)^{1/3} \quad (12)$$

Eq. (12) can be used to calculate the thickness of an adsorbed layer of liquid on a superheated,  $(T_{lv} - T_v)$ , solid surface from the value of the heat of vaporization of the liquid film,  $\Delta h$ , and the Hamaker constant,  $A$ . Conversely, the Hamaker constant can be obtained by measuring,  $\delta(T_{lv}, T_v)$ .

For small changes in the fugacity in a range where the fugacity can be replaced by the vapor pressure, Eqs. (7 and 9) give on integration with  $(\Delta n)^{-1} = -V_l$

$$P_{lv} - P_v = - \frac{V_l \Pi P_v}{RT_{lv}} + \frac{P_v V_l \Delta h}{RT_{lv} T_v} (T_{lv} - T_v) \quad (13)$$

In this equation,  $P_v$  is a reference vapor pressure of a thick, flat, liquid film,  $\Pi \rightarrow 0$ , with a surface temperature  $T_{lv} = T_v$  and  $\Delta h$  is the ideal heat of vaporization of the film. Equation (13) can be modified to include curvature at the liquid vapor interface by replacing  $\Pi$  by  $\Pi + \sigma_{lv}K$  in which  $K$  is the curvature and  $\sigma_{lv}$  is the surface tension of the liquid-vapor interface:

$$P_{lv} - P_v = - \frac{V_l P_v}{RT_{lv}} (\Pi + \sigma_{lv}K) + \frac{P_v V_l \Delta h}{RT_{lv} T_v} (T_{lv} - T_v) \quad (14)$$

Equation (14) also represents the change in equilibrium vapor pressure relative to the pool surface of the extended meniscus presented in Figure (1) for a change in temperature of  $(T_{lv} - T_v)$  and hydrostatic pressure equal to  $\rho_l g x \approx (\Pi + \sigma_{lv}K)$ . This is



approximate since buoyancy has been neglected. An integration in the vapor space at constant  $T_v$  gives for small changes in the vapor pressure

$$P_{vx} - P_v = - \frac{MgP_v x}{RT_v} \quad (15)$$

Combining Eqs. (14 and 15) with  $P_{vx} = P_{lv}$  gives for the equilibrium case

$$P_{lv} - P_{vx} = - \frac{V_l P_v}{RT_{lv}} (\Pi + \sigma_{lv} K) + \frac{MgP_v}{RT_v} x + \frac{P_v V_l \Delta h}{RT_{lv} T_v} (T_{lv} - T_v) = 0 \quad (16)$$

For  $T_{lv} = T_v$ , this reduces to the identity

$$V_l (\Pi + \sigma_{lv} K) = V_l \rho_l g x = (Mgx)_l = (Mgx)_v \quad (17)$$

If  $P_{vx} \neq P_{lv}$ , Eq. (16) can be used along with kinetic theory to calculate the rate of evaporation from (or condensation on) a curved thin film as demonstrated in the next section.

#### Interfacial mass flux.

In 1953 Schrage [17] reviewed the literature, presented and discussed the following equation based on kinetic theory relating the net mass flux of matter crossing a liquid-vapor interface to a jump change in interfacial conditions at the interface:

$$\dot{m} = C_1 \left( \frac{M}{2\pi R} \right)^{1/2} \left( \frac{P_{lv}}{T_{lv}^{1/2}} - \frac{P_v}{T_v^{1/2}} \right) \quad (18)$$

Herein, we presume that the net mass flux crossing the interface (e.g., evaporation) results from a small vapor pressure drop across an imaginary plane at the interface in which  $P_{lv}$  is the quasi-equilibrium vapor pressure of the liquid film at  $(T_{lv}, K, \Pi, x)$  and  $P_{vx}$  is the equilibrium vapor pressure of a reference bulk liquid ( $K = 0, \Pi = 0, x$ ) at a temperature  $T_v$ . Neglecting resistances in the bulk vapor space,  $P_{vx}$  and  $T_v$  can exist at a short distance from the interface, and a resistance to evaporation at the interface can be defined using Eq. (18). Using  $T_{lv}^{1/2} = T_v^{1/2}$ , this can be rewritten as

$$\dot{m} = C_1 \left( \frac{M}{2\pi R T_i} \right)^{1/2} (P_{lv} - P_{vx}) \quad (19)$$

Wayner, et al. [11] used an extended Clapeyron equation for the variation of equilibrium vapor pressure with temperature and disjoining pressure in a horizontal thin film to obtain Eq. (20) for the vapor pressure difference in Eq. (19).

$$P_{lv} - P_{v0} = \frac{P_v M \Delta h_m}{RT_v T_{lv}} (T_{lv} - T_v) + \frac{V_l P_v}{RT_{lv}} (P_l - P_v) \quad (20)$$

We note that, when interfacial effects are important, the effective pressure in the liquid,  $P_l$ , is not necessarily equal to the pressure in the vapor or to its normal vapor pressure. For example, the equilibrium vapor pressure of a small droplet is not the same as that of a flat pool of bulk liquid at the same temperature, and the pressure inside the droplet is greater than the surrounding pressure because of surface tension. The concept of pressure is further clouded by the concept of internal pressure due to cohesion which is extended in thin films to include adhesion. Therefore,  $P_{lv}$  is used to designate the equilibrium vapor pressure of an interface at  $T_{lv}$  changed by interfacial forces and  $(P_l - P_v)$  designates the pressure change in the liquid due to interfacial forces. For example, the above equation can be used to calculate the required subcooling needed to achieve equilibrium between a curved interface (droplet) and a flat interface when the vapor pressure is changed by surface tension.

Combining Eqs. (19 & 16) gives for the non-equilibrium case

$$\dot{m} = C_1 \left( \frac{M}{2\pi RT_i} \right)^{1/2} \left\{ \frac{P_v M \Delta h_m}{RT_v T_{lv}} (T_{lv} - T_v) - \frac{V_l P_v}{RT_{lv}} (\Pi + \sigma_{lv} K) + \frac{MgP_v}{RT_v} x \right\} \quad (21)$$

which can be used to calculate the interfacial mass flux.

Herein, there are two interfacial effects that can cause an effective pressure jump at the liquid-vapor interface: capillarity,  $\sigma_{lv} K$ , and disjoining pressure,  $\Pi$ . The significance of the disjoining pressure herein is that the vapor pressure of an adsorbed completely wetting liquid film is reduced by interfacial forces and therefore a superheated adsorbed liquid film can exist in (vapor pressure) equilibrium with a bulk liquid at a lower temperature. For convenience, we will emphasize spreading (zero contact angle) fluids and will use the following sign convention

$$P_l - P_v = -\sigma_{lv} K - \Pi \quad (22)$$

$$\Pi \approx -\frac{B}{\delta^n} = -\frac{\dot{A}}{\delta^3} \quad (23)$$

The approximation,  $n = 3$ , in Eq. (23) restricts its use to thicknesses  $\delta \lesssim 20$  nm. However, in the numerical examples presented below this is acceptable because either  $\delta \lesssim 20$  nm or  $\Pi \approx 0$ . The equations can be easily modified for general use and/or for other cases. It is useful to make the mass flux dimensionless using an ideal mass flux based on the temperature change only:

$$\dot{m}^{id} = C_1 \left( \frac{M}{2\pi RT} \right)^{1/2} \left( \frac{P_v M \Delta h_m}{RT_v T_{lv}} \right) (T_{lv} - T_v) \quad (24)$$

$$\dot{M} \equiv \frac{\dot{m}}{\dot{m}^{id}} = 1 - \frac{V_l T_i}{M \Delta h_m \Delta T} (\sigma_{lv} K + \Pi - \rho_l g x) \quad (25)$$

with  $\Delta T = (T_{lv} - T_v)$ . Taking  $\dot{M} = 0$ ,  $n = 3$ ,  $B = \bar{A} = A/6\pi$ ,  $K = 0$  in Eq. (25), Eq. (12) for the thickness of a flat adsorbed liquid film,  $\delta_0$ , on a superheated surface with  $\Delta T_0 \equiv (T_{lv} - T_v)$  can be recovered.

Restricting the following material to a constant interfacial temperature difference,  $\Delta T_0 = (T_{lv} - T_v)$ , and defining a reference disjoining pressure,  $\Pi_0 \equiv -\bar{A}/\delta_0^3$ , Eq. (25) becomes

$$\dot{M} = 1 - (\sigma_{lv}K + \Pi - \rho_l g x) \Pi_0^{-1} \quad (26)$$

A constant temperature difference simplifies the analysis and should not alter the significance of the results. It is useful to keep in mind that  $\Pi_0$  could be replaced by the equivalent temperature difference using Eq. (12).

Using  $\eta = \delta/\delta_0$  and  $\xi = x/x_0$  the curvature,  $K$ , for small interfacial slopes, can be written as

$$K = \frac{\delta''}{[1 + (\delta')^2]^{3/2}} \approx \delta'' = \frac{\delta_0}{x_0^2} \frac{d^2\eta}{d\xi^2} \quad (27)$$

Defining the parameter  $3 Nc \equiv \sigma_{lv}\delta_0/\Pi_0 x_0^2$  with  $\Pi_0 = \eta^3 \Pi$  and  $\rho_l g x = \Pi_0 X$  gives

$$\dot{M} = 1 - 3Nc\eta'' - \eta^{-3} + X \quad (28)$$

With dimensionless terms the prime refers to differentiation with respect to  $\xi$ , otherwise  $x$ . Eq. (28) gives the change in the dimensionless evaporation rate resulting from the effects of gravity and interfacial forces on the vapor pressure. Using  $\alpha \Delta T_0 = \dot{m} \Delta h_m$ , this can also be written as a dimensionless liquid-vapor interfacial heat transfer coefficient:

$$\frac{\alpha}{\alpha_{id}} = 1 - 3Nc\eta'' - \eta^{-3} + X \quad (29)$$

Therefore, an interfacial heat transfer coefficient can be obtained from first principles. In [11] only the changes due to disjoining pressure and temperature were analyzed. Considerable insight can be obtained from Eq. (28). We find that at the leading edge of an evaporating horizontal ( $X = 0$ , due to  $g = 0$ ) flat ( $\eta'' = 0$ ) thin film,  $\eta = 1$ , the evaporation rate can be zero even through the superheat can be substantial. This condition is required to define a stationary interline for an evaporating thin liquid film with varying thickness which has an equilibrium contact angle equal to zero. The interline has been defined as the location of the junction of an evaporating thin film and a non-evaporating adsorbed film [11]. However, when the dimensionless film thickness is  $\eta = 4.6$  ( $X = 0$ ,  $\eta'' = 0$ ), the evaporation rate will be 99% of its substantial ideal value. When  $\eta < 1$ , condensation occurs. These equations allow the interfacial forces and thermal effects to be compared and combined, and have many uses in evaporating,

condensing and/or equilibrium systems.. For curvature to have the same effect, use of Eqs. (12 and 26) with  $\Pi = 0$  and  $g = 0$  gives

$$K_o = \frac{\Delta h \Delta T_o}{\sigma_{lv} T_v} \quad (30)$$

Using Eq. (12) and  $\Pi_o = \rho_l g x$ , the following equivalents are obtained for octane on  $\text{SiO}_2$  at 298.16K with  $A/6\pi = -3.18 \times 10^{-22}$  J.

$\Delta T_o$ , K	$K_o$ , $\text{m}^{-1}$	$\Pi_o$ , $\text{N/m}^2$	$\delta_o$ , nm	$x$ , m
0.1	$3.94 \times 10^6$	$8.49 \times 10^4$	1.55	12.4

This demonstrates that the decrease in film thickness associated with a  $\Delta T = 0.1$  K is equivalent to the pressure difference associated with a static liquid head of 12.4 m. This is a pressure drop available for fluid flow.

### Fluid Mechanics.

Fluid flow in a curved thin film is also controlled by the "pressure" gradient. Using the definitions for  $\eta$ ,  $\xi$ ,  $x_o$ ,  $\Pi_o$  and the small slope assumption given above leads to

$$\frac{d}{dx} (\sigma_{lv} K + \Pi - \rho_l g x) = \frac{3\Pi_o}{x_o} (Nc\eta''' - \frac{\eta'}{\eta^4} - \frac{X'}{3}) \quad (31)$$

Using the lubrication approximation while neglecting surface shear stress, the mass flow rate per unit width in a liquid film can be approximated by

$$\Gamma = -\frac{\delta^3}{3v} \frac{d}{dx} [P_l + \rho_l g x] \quad (32)$$

Using Eqs. (22, 31 and 32) while assuming  $\rho_v \ll \rho_l$  gives

$$\Gamma = \frac{\delta^3 \Pi_o}{x_o v} (Nc\eta''' - \frac{\eta'}{\eta^4} - \frac{X'}{3}) \quad (33)$$

and the following equation for the dimensionless mass flow rates in the film

$$\bar{\Gamma} \equiv \frac{\Gamma x_o v}{\delta_o^3 \Pi_o} = Nc\eta^3 \eta''' - \frac{\eta'}{\eta} - \frac{\eta^3 X'}{3} \quad (34)$$

### DISCUSSION

Using Eq. (35) for a steady state, stationary thin film with phase change

$$\frac{d\Gamma}{dx} = -\dot{m} \quad (35)$$

and Eq. (36) with Eq. (28) gives Eq. (37)

$$\frac{d\bar{\Gamma}}{d\xi} = \frac{\dot{m} x_0^2 v}{\dot{A}} = -\dot{M} \quad (36)$$

in which  $x_0^2 \equiv -\dot{A}/v \dot{m}$  id

$$\left( \frac{\eta'}{\eta} + \frac{\eta^3 X'}{3} - Nc\eta^3 \eta''' \right)' = 1 - 3Nc\eta'' - \eta^{-3} + X \quad (37)$$

Using four boundary conditions, Eq. (37) can be numerically solved to determine the heat transfer characteristics of a stationary, steady state, thin film. When the right-hand side and the left-hand side of Eq. (37) are not equal, the above material can be used with Eq. (1) to analyze the transient case.

An evaluation of Eq. (21) demonstrates that, in an isothermal horizontal ultra-thin film, evaporation or condensation occurs unless  $(\Pi + \sigma_{LV}K) = 0$ . Using simple models, this case without phase change has been previously discussed for the leading edge of a film ( $\Pi > 0$ ,  $K < 0$ ) by deGennes and Joanny [18] and for the partial wetting case ( $\Pi < 0$ ,  $K > 0$ ) by Wayner [19]. The results demonstrate that the interface becomes planar very rapidly.

For motion to occur in an isothermal, ultra-thin, horizontal film, Eq. (32) demonstrates that  $(\Pi + \sigma_{LV}K) \neq 0$ . This indicates that fluid flow due to interfacial forces in an "isothermal" thin film must be associated with change-of-phase heat transfer (Eq. (21)). Therefore, at the leading edge of a spreading ultra-thin film a small temperature gradient due to change-of-phase heat transfer is present. However, this would be extremely small with low volatile fluids. In general the temperature gradient would not effect the above analysis unless a relatively large gradient was applied.

## RELATIVE IMPORTANCE OF INTERFACIAL MASS FLUX TO LIQUID FLOW RATE GRADIENT

### Draining Vertical Thin Film

Neglecting curvature and curvature gradient terms as compared to gravity for the case of a relatively thick ( $\Pi \approx 0$ ), isothermal ( $\Delta T = 0$ ) draining film, the ratio of Eq. (21) to the derivative of Eq. (32) leads to

$$\frac{\dot{m}}{\Gamma'} = \frac{-EV/P_v v x}{RT_v \delta^2 \delta'} \quad (38)$$

in which

$$E = C_1 \left( \frac{M}{2\pi RT_i} \right)^{1/2} \quad (39)$$

For  $\delta = 10^{-6}$  m,  $x = 10^{-2}$  m with octane at 298 K ( $P_v = 14$  mmHg,  $E_v = 4 \times 10^{-9}$  m), we find

$$\frac{\dot{m}}{\Gamma'} \approx \frac{4.8 (10^{-3})}{\delta'} \quad (40)$$

Recent studies of draining liquid films of octane found that  $\delta' \approx 6 \times 10^{-3}$  at  $x = 10^{-2}$  m when  $\delta = 10^{-6}$  m [20]. Therefore, both evaporation and liquid flow would effect the rate of decrease of film thickness for these conditions. In these studies, the films were observed to drain faster than that anticipated due to gravitational forces only. Additional interfacial effects due to  $(\sigma_{LV}K)'$  were also probably present. Further, this ratio and those discussed below do not include the resistance to diffusion in the vapor space.

#### Spreading Horizontal Film in the Region $\delta \rightarrow 0$ (Contact Line Motion)

For the case of a horizontal ( $g=0$ ) isothermal ( $\Delta T \approx 0$ ), spreading ( $\Pi = -\lambda/\delta^3$ ), slightly tapered ultra-thin film, Eqs. (21, 22, and 32) with  $\Pi \gg \sigma K$  and  $(\sigma K)' = 0$  gives

$$\frac{\dot{m}}{\Gamma'} = \frac{EV_L P_{vV}}{RT_{LV} \delta [\delta \delta'' - (\delta')^2]} \quad (41)$$

For octane at 298 K with  $\delta = 10^{-9}$  m,  $\delta' \sim 10^{-6}$ ,  $\delta'' \sim 10^{-3} \text{ m}^{-1}$ ,  $[\delta \delta'' - (\delta')^2]$  is of the order  $10^{-12}$ , and

$$\frac{\dot{m}}{\Gamma'} = \frac{4.9 \times 10^{-13}}{(10^{-9})(10^{-12})} \sim 0(10^8) \quad (42)$$

It appears that contact line motion is primarily due to an evaporation/condensation mechanism for these conditions. Once a change of phase occurs,  $\Delta T \neq 0$ , and the value of the ratio in Eq. (42) would decrease. However, this would not affect the basic conclusion. Although an additional resistance due to diffusion would be present with a non-condensing second component in the vapor, the diffusion path length can be extremely small. We note that Hardy and Doubleday found that primary film spreading was a function of molecular weight and vapor pressure when the fluids had a sensible vapor pressure [2].

#### Contact Line Heat Sink

Using  $\Gamma = \rho \delta V$  to define an average velocity in the film, Eq. (32) and the above assumptions ( $g = 0$ ,  $K = 0$ ) lead to

$$V = \frac{\dot{A} \delta'}{\mu \delta^2} \quad (43)$$

Using the value  $\delta' = -10^{-6}$  obtained above with  $\bar{A} = -3.18 \times 10^{-22}$  J (octane -  $\text{SiO}_2$ ),  $\mu = 5.16 \times 10^{-4}$  N·s/m<sup>2</sup> and  $\delta = 10^{-9}$  m in Eq. (43) gives  $V = 6.1 \times 10^{-7}$  m/s for perspective.

Assuming that all the liquid which flows through a plane perpendicular to the substrate at a given location evaporates in the thinner portion of a steady state, stationary film with  $\Delta T > 0$ , a contact line heat sink can be defined as

$$Q = \Gamma \Delta h_m = \frac{\bar{A} \delta' \Delta h_m}{v \delta} \quad (44)$$

Therefore, it is possible to obtain the contact line heat sink knowing the thermophysical properties, the maximum thickness of the region and the slope at this thickness. The slope is a measure of the departure from equilibrium leading to fluid flow; the temperature difference and reference condition indicate whether or not phase change occurs.

#### Spreading Horizontal Film (Incomplete Wetting)

The following simple model has been used to describe the contact line region of an equilibrium liquid film with a finite contact angle [19].

$$\Pi + \sigma_{lv} K = 0 \quad (45)$$

In this case  $\Pi < 0$  and  $K > 0$ , or we might say that the disjoining pressure increases the vapor pressure and the curvature decreases the vapor pressure. Since fluid motion in the liquid film would result from an increase in the curvature gradient, this curvature change would also lead to condensation and a change in the apparent contact angle. The processes can be separated only by degree of importance.

#### CONCLUSION

The physical phenomena associated with spreading have been extensively addressed using various models for low vapor pressure fluids (e.g., see the reviews by deGennes [21], Cazabat [22], and Neogi and Miller [9]). They range from the rolling motion observed by Dussan and Davis [23] to the surface diffusion model discussed by Ruckenstein and Dunn [24]. As demonstrated above, change of phase heat transfer is also important for many conditions. Bascom, et al. [6] citing deBoer [25] noted that surface diffusion can be energetically more favorable than evaporation. Indeed, deBoer [25] discussed this situation for the case of a two-dimensional gas. He also noted that lateral migration would be restricted when two-dimensional condensation occurred. Additional research on spreading as a function of film thickness is warranted. In general, the non-equilibrium processes of fluid flow and change of phase heat transfer are intrinsically connected because of their common dependence on the intermolecular force field and gravity. The relative importance of the various mechanisms depend on the physical properties of ultra-thin films and how they are effected by pressure, (i.e., cohesion, adhesion, thickness, curvature) and temperature.

## REFERENCES

1. J.S. Rowlinson and B. Widom, *Molecular Theory of Capillarity*, Clarendon Press, Oxford, 1982.
2. W.B. Hardy and I. Doubleday, *Proc. Roy. Soc. Ser. A*, 100 (1922) 550-574.
3. B. V. Derjaguin, *Acta Physicochimica URSS (Eng. Trans.)* XII (2) (1940) 181-200.
4. B. V. Derjaguin and L. M. Shcherbakov, *Colloid Journal USSR (Eng. Trans.)* 23 (1961) 33-44.
5. B. V. Derjaguin and Z. M. Zorin, *Zh. Fiz. Khim.*, 29 (1955) 1010 & 1755.
6. W.D. Bascom, R.L. Cottingham and C.R. Singleterry, in *Contact Angle R.E.*, Gould, ed., *Advances in Chemistry Series*, Am. Chem. Soc., Washington, D.C., 43 (1964) 355-379.
7. J.A. de Feijter in I.B. Ivanov (Ed.) *Thin Liquid Films, Fundamentals and Applications*, Marcel Dekker, Inc., New York, 1988, pp 1-47.
8. I.B. Ivanov and D.S. Dimitrov in I.B. Ivanov (Ed.) *Thin Liquid Films, Fundamentals and Applications*, Marcel Dekker, Inc., New York, 1988, pp 379-496.
9. P. Neogi and C.A. Miller, *A.I.Ch.E. Symposium Series*, 252 (82) (1988) 145-155.
10. M. Potash, Jr. and P.C. Wayner, Jr., *Int. J. Heat Mass Transfer*, 15 (1972) 1851-1863.
11. P. C. Wayner, Jr., Y. K. Kao and L. V. La Croix, *Int. J. Heat Mass Transfer*, 19 (1976) 487-492.
12. V. Ludviksson and E.N. Lightfoot, *A.I.Ch.E. Journal*, 14 (1968) 674-677.
13. C. Huh and L.E. Scriven, *J. Colloid Interface Sci.*, 35 (1971) 85-101.
14. C.A. Miller and E. Ruckenstein, *J. Colloid Interface Sci.*, 48 (1974) 368-
15. C.J. Parks and P.C. Wayner, Jr., *AIChE Journal*, 33 (1987) 1-10.
16. G.F. Teletzke, H.T. Davis, and L.E. Scriven, *Chem. Eng. Comm.*, 55 (1987) 41-81.
17. R.W. Schrage, *A Theoretical Study of Interphase Mass Transfer*, Columbia University Press, New York, NY, 1953.
18. J.F. Joanny and P.G. deGennes, *J. Colloid Interface Sci.*, 111 (1986) 94-101.
19. P.C. Wayner, Jr., *J. Colloid Interface Sci.*, 88 (1982) 294-295.



20. M. Sujanani and P.C. Wayner, Jr., to be published in Proceedings of 4th EPS Liquid State Conference on Hydrodynamics of Dispersed Media, Arcachon, France, May 24-27, 1988.
21. P.G. deGennes, *Rev. Mod. Phys.*, 57 (1985) 827-863.
22. A.M. Cazabat, *Contemp. Phys.* 28 (1987) 347-364.
23. E.B. Dussan V. and S.H. Davis, *J. Fluid Mech.*, 65 (1974) 71-96.
24. E. Ruckenstein and C.S. Dunn, *J. Colloid Interface Sci.*, 39 (1977) 135-138.
25. J.H. deBoer, *The Dynamical Character of Adsorption*, Oxford University Press, London, 1953.

#### ACKNOWLEDGEMENT

This material is based on work supported by the Aero Propulsion Laboratory, Air Force Wright Aeronautical Laboratory, Aeronautical Systems Division (AFSC), United States Air Force, Wright-Patterson AFB, Ohio 45433-6563 under contract F33615-88-C-2821. The U.S. Government is authorized to reproduce and distribute reprints for governmental purposes notwithstanding any copyright notation. Any opinions, findings, and conclusions or recommendations expressed in this publication are those of the author and do not necessarily reflect the view of the U.S. Air Force.

## NOMENCLATURE

A	= Hamaker constant ( $6\pi\text{\AA}$ )
C	= condensation coefficient
f	= fugacity
g	= acceleration due to gravity
h	= enthalpy/ volume, heat transfer coefficient
K	= curvature
M	= molecular weight
m	= interfacial mass flux
n	= molar density
P	= pressure
R	= gas constant
s	= entropy/volume
T	= temperature
t	= time
V	= molar volume
X	= dimensionless position
$\alpha$	= interfacial heat transfer coefficient
$\Delta$	= difference
$\delta$	= film thickness
$\Gamma$	= mass flow rate / width
$\gamma$	= film tension
$\eta$	= dimensionless thickness
$\mu$	= chemical potential/mole, dynamic viscosity
$\nu$	= kinematic viscosity
$\Pi$	= disjoining pressure
$\rho$	= density
$\sigma$	= interfacial tension
$\xi$	= dimensionless position

### subscripts

g	= includes gravity
i	= average value
l	= liquid
lv	= liquid-vapor interface
m	= unit mass
T	= tangential
v	= vapor
x	= at x

### superscripts

id	= ideal
', "	= derivatives

APPENDIX B

HEAT TRANSFER AND FLUID FLOW IN AN  
EVAPORATING EXTENDED MENISCUS

# HEAT TRANSFER AND FLUID FLOW IN AN EVAPORATING EXTENDED MENISCUS

P.C. Wayner, Jr. and J. Schonberg

Department of Chemical Engineering  
Rensselaer Polytechnic Institute  
Troy, N.Y. 12180

The rate of evaporation from a steady extended meniscus formed between the exits of two facing slot feeders is analyzed. The meniscus is symmetric about the centerplane. The physicochemical phenomena associated with cohesion and adhesion at interfaces are used to formulate transport equations unique to evaporating thin films which are then numerically solved for two types of menisci. One type involves an adsorbed thin film dominated by disjoining pressure effects, a thicker portion dominated by capillary effects and a transition region between. The second type has no thin film portion; the transition region straddles the plane of symmetry. In a sample calculation the heat flux is found to be roughly nine times higher for the latter type of meniscus. For the conditions studied, we find that a smaller value of the Hamaker constant (weaker adsorption) leads to an increase in the relative importance of capillarity and to a higher evaporation rate.

## 1. INTRODUCTION

Fluid flow and evaporation in an extended meniscus that includes both a relatively thick region controlled by capillarity and an ultra-thin region controlled by the liquid-solid-vapor interfacial force field (disjoining pressure) is of importance to many heat transfer processes. When the film thickness is less than  $10^{-7}$  m, long range intermolecular forces start to affect the pressure distribution in the liquid and its vapor pressure. For fluids that completely wet the substrate, these effects are, of course, extremely small for thicknesses of the order of  $10^{-7}$  m. However, they become the predominant effect as the film becomes ultra-thin. Herein, we evaluate these complementary effects.

Derjaguin et al. (e.g. 1957, 1965) laid the foundation for the study of the mechanics and thermodynamics of ultra-thin films when they measured the thickness of an adsorbed liquid film on a superheated substrate, discussed the flow of an evaporating ultra-thin film in a capillary and defined the disjoining pressure to account for the modified force field in the liquid. Potash and Wayner (1972) used these concepts to describe evaporation from a stationary, steady-state, evaporating extended meniscus on a vertical flat plate. Miller (1973) studied

the stability of moving liquid-vapor interfaces as a result of phase change. Wayner et al. (1976) used an extended Clausius-Clapeyron equation to define an interline heat transfer coefficient. In 1979 these concepts were used to model evaporation from grooves (Holm and Goplen (1979)). Moosman and Homsy (1980) used perturbation theory to describe the profile change of an evaporating extended meniscus relative to the static isothermal profile. The thermal resistance of the liquid itself was included. The heat flux was found to be a maximum in the transition region. In the capillary region (for the particular parameters chosen) the film resistance hindered evaporation. In the thin adsorbed film disjoining pressure hindered evaporation. Herein, film resistance is neglected; however the fully non-linear equations are numerically analyzed; thus the heat flux may be larger than in the linearized process (Moosman and Homsy, 1980). Furthermore in this work the meniscus need not terminate in an adsorbed thin film.

Studies by Parks and Wayner (1987) and Mirzamoghadam and Catton (1988) extended the literature to include other effects (e.g. surface shear). Mirzamoghadam and Catton (1988) considered an evaporating meniscus attached to a heated plate partially immersed in a liquid pool at various angles. An approximate integral analysis was employed to study the whole process from the adsorbed thin film to the region of natural convection. Furthermore the influence of temperature on surface tension was considered. Like Moosman and Homsy (1980) the resistance of the meniscus to thermal conduction was

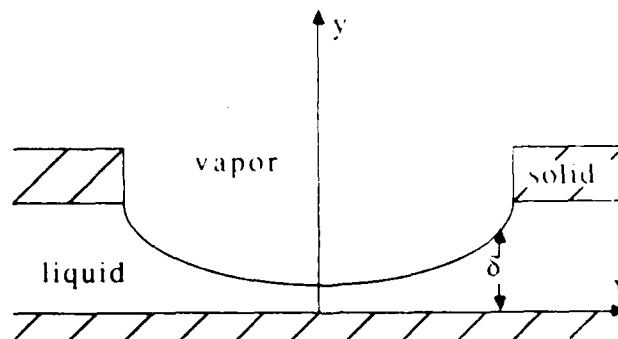


Figure 1 Symmetric meniscus between two feed ports.

included. Das and Gaddis (1987) evaluated the pressure distribution near an evaporating contact line. Herein, we apply these concepts to a new meniscus configuration (Fig. 1) which naturally leads to the evaluation of important new boundary conditions in the numerical solution of the full non-linear equation for an evaporating single component film with a constant surface temperature. The basic equations are reformulated so that a dimensionless group,  $N_c$ , represents the relative importance of capillarity to a reference disjoining pressure which, in turn, is a function of the substrate superheat.

## 2. THEORETICAL BACKGROUND

2.1 Interfacial mass flux: Schrage (1953) reviewed the literature, and presented and discussed Eq. (1) based on kinetic theory relating the net mass flux of matter crossing a liquid-vapor interface to a jump change in interfacial conditions at the interface:

$$\dot{m} = C_1 \left( \frac{M}{2\pi R} \right)^{1/2} \left( \frac{P_{lv}}{T_{lv}^{1/2}} - \frac{P_v}{T_v^{1/2}} \right) \quad (1)$$

The net mass flux across the interface results from a small vapor pressure drop across an imaginary plane at the interface in which  $P_{lv}$  is the equilibrium vapor pressure of the bulk liquid at  $T_{lv}$ , and  $P_v$  is the equilibrium vapor pressure of the reference bulk liquid at a temperature  $T_v$ . Neglecting resistances in the bulk vapor space,  $P_v$  and  $T_v$  can exist at a short distance from the interface, and a resistance to evaporation at the interface can be defined using Eq. (1). Using  $T_{lv}^{1/2} = T_v^{1/2}$ , this can be rewritten as

$$\dot{m} = C_1 \left( \frac{M}{2\pi R T} \right)^{1/2} (P_{lv} - P_v) \quad (2)$$

Wayner et al. (1976) used an extended Clapeyron equation for the variation of equilibrium vapor pressure with temperature and pressure to obtain Eq. (3) for the vapor pressure difference in which  $P_{v/lv}$  replaces  $P_{lv}$

$$P_{v/lv} - P_v = \frac{P_v M \Delta h}{R T_v T_{lv}} (T_{lv} - T_v) + \frac{V_l P_v}{R T_{lv}} (P_l - P_v) \quad (3)$$

in which  $\Delta h$  is the heat of vaporization of the film and  $V_l$  is the molar volume.

We note that, when interfacial effects are important, the "pressure",  $P_l$ , in the liquid is not necessarily equal to the pressure in the vapor or to its normal vapor pressure. For example, the equilibrium vapor pressure of a small droplet is not the same as that of a flat pool of bulk liquid at the same temperature and the pressure inside the droplet is greater than the surrounding pressure because of surface tension. The concept of pressure is further clouded by the concept of internal pressure due to cohesion which is extended to include adhesion herein. Therefore,  $P_{v/lv}$  is used to designate the equilibrium vapor pressure of an interface at  $T_{lv}$  affected by interfacial forces.

Equation (3) can be used to calculate the required subcooling needed to achieve equilibrium between a curved interface (droplet) and a flat interface when the vapor pressure is changed by surface tension. Combining Eqs. (2) & (3) gives the interfacial mass flux as

$$\dot{m} = C_1 \left( \frac{M}{2\pi R T} \right)^{1/2} \left\{ \frac{P_v M \Delta h}{R T_v T_{lv}} (T_{lv} - T_v) + \frac{V_l P_v}{R T_{lv}} (P_l - P_v) \right\} \quad (4)$$

Herein, there are two interfacial effects that can cause a pressure jump at the liquid-vapor interface: capillarity,  $\gamma K$ , and disjoining pressure,  $\Pi$ . A recent review article (Ivanov, 1988) describing the concepts is available. The significance of the disjoining pressure herein is that the vapor pressure of an adsorbed liquid film is reduced (complete wetting case) by interfacial forces and therefore a superheated adsorbed liquid film can exist in (vapor pressure) equilibrium with a bulk liquid at a lower temperature. For convenience, we will only look at spreading (zero contact angle) fluids herein and will use the sign convention

$$P_l - P_v = -\gamma K - \Pi \quad (5)$$

$$\Pi \approx -\frac{B}{\delta^n} = -\frac{\dot{A}}{\delta^3}, \quad \dot{A} = \frac{A}{6\pi} < 0 \quad (6)$$

in which  $A$  is the Hamaker constant,  $K$  the curvature,  $\gamma$  the surface tension and  $\delta$  the film thickness.

The approximation,  $n = 3$ , used in Eq. (6) restricts the use of Eq. (6) to thicknesses  $\delta \leq 20$  nm (Truong and Wayner, 1988). However, the numerical examples presented below demonstrate that this is acceptable for some cases in which  $\gamma K$  becomes dominant before this thickness. Further, the equations can be modified for general use for other cases. It is useful to make the mass flux dimensionless using an ideal mass flux based on the temperature change only:

$$\dot{m}_{id} = C_1 \left( \frac{M}{2\pi R T} \right)^{1/2} \left( \frac{P_v M \Delta h}{R T_v T_{lv}} (T_{lv} - T_v) \right) \quad (7)$$

$$\dot{M} \equiv \frac{\dot{m}}{\dot{m}_{id}} = 1 - \frac{V_l T_v}{M \Delta h \Delta T} (\gamma K + \Pi) \quad (8)$$

with  $\Delta T_0 = (T_{lv} - T_v)$ . Taking  $\dot{M} = 0$ ,  $n = 3$ ,  $B = \dot{A}$ ,  $K = 0$  in Eq. (8), the thickness  $\delta_0$  of a flat adsorbed liquid film on a superheated surface can be obtained:

$$\delta_0 = \left( \frac{-V_l T_v \dot{A}}{M \Delta h \Delta T_0} \right)^{1/3} \quad (9)$$

Restricting the following material to a constant interfacial temperature difference,  $\Delta T_0$  and defining a reference disjoining pressure,  $\Pi_0 =$

$-\dot{A}/\delta_0^3$ , Eq. (8) becomes

$$\dot{M} = 1 - (\gamma K + \Pi) \Pi_0^{-1} \quad (10)$$

Using  $\eta = \delta/\delta_0$  and  $\xi = x/x_0$  the curvature,  $K$ , for small interfacial slopes, can be written as

$$K = \frac{\delta''}{[1 + (\delta')^2]^{3/2}} \approx \delta'' = \frac{\delta_0}{x_0^2} \frac{d^2\eta}{d\xi^2} \quad (11)$$

Defining the parameter  $3 N_c \equiv \gamma\delta_0/\Pi_0 x_0^2$  with  $\Pi_0 = \eta^3 \Pi$  gives

$$\dot{M} = 1 - 3N_c \eta'' - \eta^{-3} \quad (12)$$

Eq. (12) gives the reduction in the evaporation rate resulting from the effect of interfacial forces on the vapor pressure. Using  $\alpha\Delta T_0 = \dot{m}\Delta h$ , this can also be written as a dimensionless liquid-vapor interfacial heat transfer coefficient:

$$\frac{\alpha}{\alpha_{id}} = 1 - 3N_c \eta'' - \eta^{-3} \quad (13)$$

Considerable insight can be obtained from Eq. (12). Consider two hypothetical menisci. Each is a perfectly flat film, one is deeper ( $\eta = 4.6$ ) and one is shallower ( $\eta = 1.0$ ). Each is superheated; however, there is no evaporation from the latter meniscus due to adsorption. However the evaporation rate from the former meniscus is 99% of its ideal value. For curvature alone to prevent evaporation it must be equivalent:

$$K_0 = \frac{M\Delta h\Delta T_0}{\gamma V_l T_v} \quad (14)$$

This follows from Eqs. (9) and (10) and the requirement.

**2.2 Fluid Mechanics:** Fluid flow in a curved thin film is also controlled by the pressure along the interface. Using the definitions for  $\eta$ ,  $\xi$ ,  $x_0$ ,  $\Pi_0$  and the small slope assumption given above leads to

$$\frac{d}{dx} (\gamma K + \Pi) = \frac{3\Pi_0}{x_0} (N_c \eta''' - \frac{\eta'}{\eta^4}) \quad (15)$$

Using the lubrication approximation, the mass flow rate  $\Gamma$  per unit width in a slightly tapered liquid film can be written as

$$\Gamma = -\frac{\delta^3}{3\nu} \frac{dP_l}{dx} \quad (16)$$

in which  $\nu$  is the kinematic viscosity.

Using Eqs. (5, 15 and 16) while assuming a constant pressure in the vapor gives

$$\Gamma = \frac{\delta^3 \Pi_0}{x_0 \nu} (N_c \eta''' - \frac{\eta'}{\eta^4}) \quad (17)$$

from which follows the dimensionless mass flow rate in the film

$$\bar{\Gamma} \equiv \frac{\Gamma x_0 \nu}{\delta_0^3 \Pi_0} = N_c \eta^3 \eta''' - \frac{\eta'}{\eta} \quad (18)$$

Using

$$\frac{d\bar{\Gamma}}{d\xi} = -\dot{m} \quad (19)$$

and

$$\frac{d\bar{\Gamma}}{d\xi} = \frac{\dot{m} x_0^2 \nu}{A} = -\dot{M} \quad (20)$$

in which  $x_0^2 \equiv A/\nu \dot{m}$  and, with Eq. (12) gives

$$(\frac{\eta'}{\eta} - N_c \eta^3 \eta''')' = 1 - 3N_c \eta'' - \eta^{-3} \quad (21)$$

The lefthand side of Eq. (21) represents fluid flow and the righthand side represents interfacial mass flow.

### 3. RESULTS AND DISCUSSION

**3.1 Numerical:** In principle the descriptive Eq. (21) may be solved as written, however, the parameter  $N_c$  may be small. In that case the highest order derivative is multiplied by a small parameter which creates numerical difficulties. This problem was avoided by rescaling the dimensionless distance. A new distance  $\lambda$  is thus defined according to

$$\lambda = \frac{\xi}{N_c^{1/2}} \quad (22)$$

The transformed differential equation is

$$(\frac{\eta'}{\eta} - \eta^3 \eta''')' = N_c (1 - 3\eta'' - \eta^{-3}) \quad (23)$$

where the superscript prime now refers to differentiation by  $\lambda$ .

Applying the transformation, Eq. (22), to the expression for the total mass flow rate in the film, Eq. (18), yields

$$\bar{\Gamma} = \frac{1}{N_c^{1/2}} (\eta^3 \eta''' - \frac{\eta'}{\eta}) \quad (24)$$

where the superscript prime denotes differentiation by  $\lambda$ . If the meniscus is symmetric, at the symmetry plane,  $\lambda = 0$ , the mass flow rate  $\bar{\Gamma}$  must be equal to zero with

$$\eta''' = 0 \text{ and } \eta' = 0 \quad (25)$$

Equation (25) provides two of the necessary four initial conditions. The values of  $\eta$  and  $\eta''$  at the center plane are parameters.

$$\eta = \eta_0 \quad \lambda = 0 \quad (26)$$

$$\eta'' = \eta''_0 \quad \lambda = 0 \quad (27)$$

These initial conditions are different from the corresponding conditions used in previous studies which considered a meniscus beginning with an adsorbed, non-evaporating thin film (i.e.,  $\eta(0) = 1$ ). First, Gear's method was applied to the differential equation (23) and boundary conditions, Eqs. (25-27), for a given value of  $N_c$ , but various values of the initial conditions were selected. This allows comparison of a meniscus with a small adsorption effect at the origin (Case A,  $\eta(0) = 4$ ) to those previously analyzed with a large adsorption effect (Case B,  $\eta(0) = 1.02$ ). The dimensionless meniscus thickness profile and dimensionless evaporation flux profile are displayed in Figures 2 and 3. These figures suggest that a cooling device using a meniscus between two feed ports (Figure 1) with a minimum adsorption effect at the centerplane would provide a heat flux several times larger than a device employing a meniscus which terminates in a thin adsorbed film. In the case at hand the heat flux is roughly 8.8 times larger. This result reinforces the view that, whereas the adsorption effects are necessary to keep the film in contact with the substrate at the origin, they reduce the heat flux. Further, the pressure gradient is much greater in the thinner films. In both cases the evaporation rate is fairly constant. However in case A  $\eta^{-3}$  is never very large whereas in case B  $\eta^{-3}$  starts near one and decreases to near zero. Therefore Equation 12 shows that the curvature will vary weakly in case A but strongly in case B. In case B it increases with increasing  $\lambda$  and then decreases slightly. The increase is clearly shown by Figure 2.

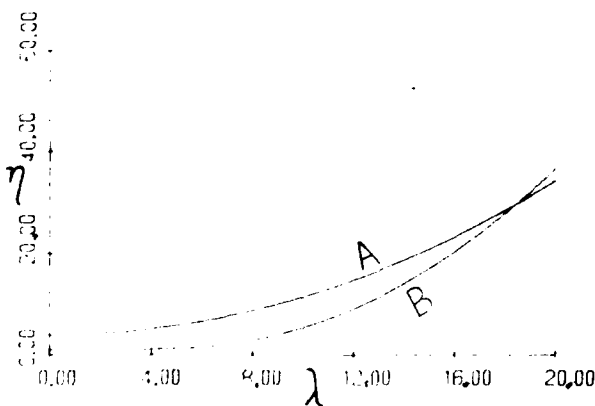


Figure 2 Dimensionless plot of film thickness versus distance for two types of meniscus. In Case A  $\eta_0 = 4.0$  and  $\eta''_0 = 0.15$  whereas in Case B  $\eta_0 = 1.02$  and  $\eta''_0 = 0.005$ . In each case  $N_c = 0.01$ .

A comparison was also developed between solutions having different values of  $N_c$  but the same values of the initial conditions (dimensionless). These dimensional solutions are shown in Figures 4-6 for the meniscus thickness, curvature, and heat flux profiles for the example system of n-octane on silicon dioxide. The dimensional pressure at the centerplane is the same in each case. The applicable values of the physical properties and groups are given in Table I.

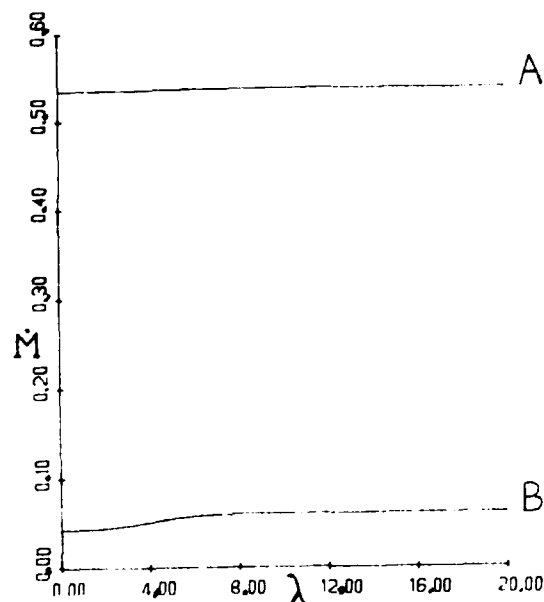


Figure 3 Dimensionless plot of evaporative flux comparing Case A with Case B

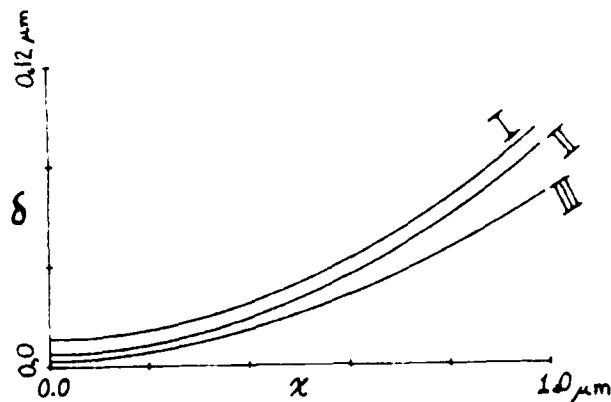


Figure 4 Dimensional plot of film thickness versus distance for Case I, II, and III (see Table I). In each case  $\eta_0 = 4.0$  and  $\eta''_0 = 0.25$ .

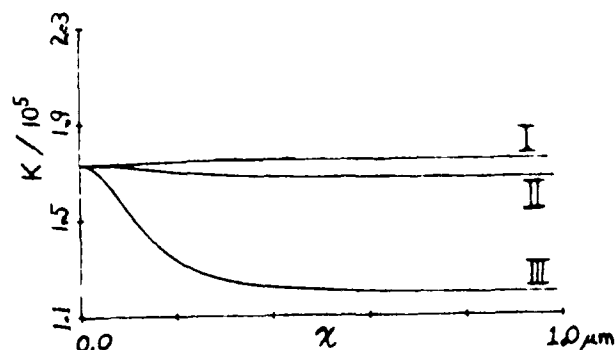


Figure 5 Dimensional plot of curvature versus distance for Case I, II, and III.

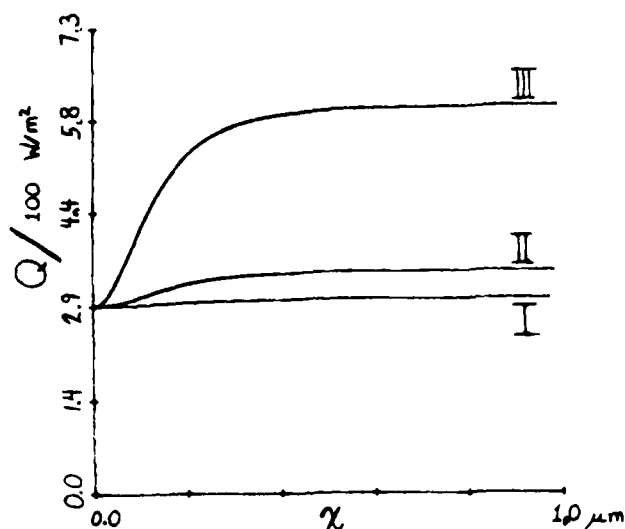


Figure 6 Dimensional plot of heat flux versus distance for Case I, II, and III.

Three different values of the Hamaker constant were assumed because it would represent a major variable in real systems. The value of the Hamaker constant has been calculated and measured for octane on  $\text{SiO}_2$  [Ingram, 1974; Truong and Wayner, 1987]. Due to contamination (e.g., an adsorbed water film) and/or a slightly microporous surface the experimental values have been found to be the lesser. Therefore, the theoretical values used in our numerical work which lead to the variation in  $N_c$  covered this range. The results in Figure 4 demonstrate how the film starts thinner with the lower value of the Hamaker constant. Figure 5 demonstrates that there is an increase in the curvature gradient and, therefore the interfacial mass flux with a decrease in the value of the Hamaker constant. This result can be described using Eq. (8): as the value of the disjoining pressure

TABLE I

CASE	I	II	III
A, J	-10 <sup>-22</sup>	-10 <sup>-23</sup>	-10 <sup>-24</sup>
F, K	298	298	298
ΔT, °C	0.00577	0.00577	0.00577
$\eta, \frac{\text{N}\cdot\text{s}}{\text{m}^2}$	5160 (10 <sup>-7</sup> )	5160 (10 <sup>-7</sup> )	5160 (10 <sup>-7</sup> )
$\rho, \text{kg/m}^3$	698.2	698.2	698.2
$P_v, \text{N/m}^2$	1.864 (10 <sup>3</sup> )	1.864 (10 <sup>3</sup> )	1.864 (10 <sup>3</sup> )
$\delta_0, 10^{-10}\text{m}$	27.296	12.67	5.881*
$N_c$	0.1	0.464	2.154
$\gamma, \frac{\text{N}}{\text{m}}$	21.3 (10 <sup>-3</sup> )	21.3 (10 <sup>-3</sup> )	21.3 (10 <sup>-3</sup> )
$x_0, \text{m}$	1.98 (10 <sup>-7</sup> )	6.25 (10 <sup>-8</sup> )	1.98 (10 <sup>-8</sup> )

\*Note:  $\delta_0$  is a reference thickness only and does not in general represent the exact film thickness.

and/or the capillary pressure decreases, the interfacial mass flux increases. The pressure gradient has a large effect and an increase in the value of  $N_c$  signifies an increase in the relative importance of capillarity. Because of the limitation on the range of validity of Eq. (6) lower values of the temperature difference between the liquid vapor interface and the vapor were used. These lower values increase the value of  $N_c$ , reducing the meniscus thickness in the transition region (the transition region bridges the adsorbed thin film dominated by disjoining pressure and the capillary meniscus in which the form of the disjoining pressure is immaterial). This resulted in lower values of the heat flux.

In this analysis we neglect various effects and simplify others. The temperature of the vapor liquid interface is taken to be constant. Thus surface stress due to a variation may be neglected. The accuracy of the assumption may be checked by calculating the temperature drop through the meniscus

$$q = k \frac{\Delta T}{\delta} \quad (28)$$

using  $k$  equal 0.14 W/mK. Thus a film thickness may be found at which this temperature drop is 10 percent of the temperature difference between the liquid and the vapor phases. The results for cases I, II, and III are 2760, 2410, and 1380 Angstroms. Therefore, the film resistance is apparently negligible for a meaningful portion of the capillary meniscus. However, we note that these cases were not chosen to optimize the heat flux, but to add insight to the phenomena. Other assumptions include lubrication flow, and the form of disjoining pressure. Thus the meniscus must be fairly flat and disjoining effects must be negligible where it is thicker than 200 Angstroms. Cases II and III satisfy the latter restriction but Case I is borderline. It is included to illustrate the trend. Another model is needed for thicker films (Truong and Wayner, 1987).

### 3.2 Additional Analytical Discussion

The model of Wayner et al. (1976) is herein extended to include capillary effects. The results may be compared in the adsorbed thin film portion of the meniscus. Here both models have analytical solutions which are only valid if

$$\eta \approx 1 \quad \text{and} \quad \frac{P_l - P_v}{P_0} \approx -1 \quad (29)$$

The isothermal model of Renk et al., (1978) also has an analytical solution, subject to the same conditions. In each of these three cases we impose the boundary condition

$$\eta \rightarrow 1 \quad \text{as} \quad \xi \rightarrow -\infty \quad (30)$$

Our result for the present model was developed with Eq. (21) and is

$$\eta \approx 1 + a e^{\xi/N_c^{1/2}} + b e^{\xi\sqrt{3}} \quad (31)$$



$$\frac{P_l - P_v}{P_0} \approx 3b(1 - 3N_c) e^{\xi\sqrt{3}} - 1 \quad (32)$$

$$\bar{\Gamma} \approx -3\sqrt{3} b(1 - N_c) e^{\xi\sqrt{3}} \quad (33)$$

where  $a$  and  $b$  are arbitrary constants.

The model of Wayner et al. (1976) also gives the same results as Eqs. (21), (31), (32), and (33) with the parameter " $a$ " equal to zero,  $N_c$  set equal to zero in Eqs. (32) and (33), and " $b$ " replaced by a different arbitrary constant,  $B$ . The non-evaporating meniscus (Renk et al., 1978) has an adsorbed thin film as well and its governing equation may also be analyzed. The governing equation is given by setting the righthand side of Eq. (21) equal to zero (this follows from Eq. (12) and the fact that there is no evaporation from an isothermal meniscus). Our result is Eqs. (31)-(33) with " $b$ " equal zero and " $a$ " replaced by a different arbitrary constant  $\alpha$ .

In the earlier model of Wayner et al. (1976) capillary effects were ignored. Therefore we expect this model to perform best if the parameter  $N_c$  is small. In that case the present solution for  $\eta$  will always be equal to the previous solution for  $\eta = 1$  sufficiently small because the first exponential term in Eq. (31) may be neglected in favor of the second term if  $\xi$  is sufficiently negative. Of course the more negative  $\xi$  is, the closer  $\eta$  is to 1. Under these conditions, the solution for pressure and mass flow are almost identical. The old solution is merely corrected by a term proportional to  $N_c$ . According to this result, the effect of capillarity is found to slightly reduce the pressure and the mass flow.

In general, however, the previous model and present model agree more or less depending on the ratio of  $a/b$  which is not a function of  $N_c$ . The details of the comparison are beyond the scope of this paper.

#### 4. CONCLUSION

Herein, we have demonstrated the effect that pressure and temperature can have on the heat transfer characteristics of the contact line. The effect of interfacial forces on the pressure field are modeled using the Hamaker constant ( $6\pi A$ ), surface tension, thickness, and curvature. At a given temperature, the pressure field affects the vapor pressure and therefore, the evaporation rate. In the test calculations, the evaporation rate was increased by decreasing adsorption. Since we are evaluating the effects of both long range liquid-solid intermolecular forces and liquid-vapor interfacial tension the importance of these results naturally increases as the system becomes smaller.

#### REFERENCES

Derjaguin, B.V. and Zorin, Z.M., 1957, Optical Study of the Adsorption and Surface Condensation of Vapors in the Vicinity of Saturation on a Smooth Surface, Proc. 2nd International Congress on Surface Activity (London), Vol.2, pp 145-152.

Derjaguin, B.V., Nerpin, S.V., and Churayev, N.V., 1965, Effect of Film Transfer upon Evaporation of Liquids from Capillaries, Bull. R.I.L.E.M., vol. 29, pp 93-98.

Das, S. and Gaddis, J.L., 1987, Pressure Distribution near an Evaporating Contact Line, in Nonequilibrium Transport Phenomena ed. Dobran, F., Bankoff, S.G., Chen, J.C., and El-Genk, M.S., HTD-Vol. 77, pp17-21, ASME, New York, NY.

Holm, F.W. and Goplen, S.P. 1979, Heat Transfer in the Meniscus Thin-Film Region, Trans. ASME Journal of Heat Transfer, vol. 101, pp 543-547.

Ingram, B.T., 1974, J. Chem. Soc. Faraday Trans., Vol. 70, pp. 868-880.

Ivanov, I.B. 1988, Thin Liquid Films: Fundamentals and Applications, Marcel Dekker, Inc., New York

Mirzamoghadam, A. and Catton, I. 1988, A Physical Model of the Evaporating Meniscus, ASME Journal of Heat Transfer, vol.110, pp 201-207.

Miller, C.A., 1973, Stability of Moving Surfaces in Fluid Systems with Heat and Mass Transfer, AIChE Journal, vol. 19, pp 909-915.

Moosman, S. and Homsy, G.M., 1980, Evaporating Menisci of Wetting Fluids, J. Colloid Interface Sci., vol. 73, pp 212- 223.

Parks, C. and Wayner, P.C., Jr., 1987, Surface Shear Near the Contact Line of a Binary Evaporating Curved Thin Film, AIChE Journal, Vol. 33, pp. 1-10.

Potash, M. Jr., and Wayner, P.C., Jr., 1972, Evaporation from a Two-Dimensional Extended Meniscus, Int. J. Heat Mass Transfer, vol. 15, pp 1851-1863.

Schrage, R.W. 1953, A Theoretical Study of Interphase Mass Transfer, Columbia University Press, New York, NY

Truong, J.G. and Wayner, P.C., Jr. (1987) Effect of Capillary and van der Waals Dispersion Forces on the Equilibrium Profile of a Wetting Fluid: Theory and Experiment, J. Chem. Phys., vol. 87, pp 4180-4188.

Wayner, P.C., Jr., Kao, Y.K., and LaCroix, L.V., 1976, The Interline Heat Transfer Coefficient of an Evaporating Wetting Film, Int. J. Heat Mass Transfer, vol. 19, pp 487-492.

#### ACKNOWLEDGEMENT

This material is based on work supported by the Aero Propulsion Laboratory, Air Force Wright Aeronautical Laboratory, Aeronautical Systems Division (AFSC), United States Air Force, Wright-Patterson AFB, Ohio 45433-6563 under contract F33615-88-C-2821. The U.S. Government is authorized to reproduce and distribute reprints for governmental purposes notwithstanding any copyright notation. Any opinions, findings, and conclusions or recommendations expressed in this publication are those of the authors and do not necessarily reflect the view of the U.S. Air Force.